

## Cyclic behavior of extended end-plate connections with European steel shapes

Alırıza İ. Akgönen\* Cavidan Yorgun and Cüneyt Vatanserver

*Department of Civil Engineering, İstanbul Technical University, 34469, Maslak, İstanbul, Turkey*

*(Received December 13, 2014, Revised February 07, 2015, Accepted April 27, 2015)*

**Abstract.** The aim of this experimental research is to investigate the conformity of the four-bolt unstiffened moment end-plate connections consisting of European steel sections which do not meet the limitations specified for beam flange width and overall beam depth in ANSI/AISC 358-10 to the requirements of seismic application. However, the connections are satisfactory with the limitations required by Turkish Earthquake Code. For this purpose, four test specimens were designed and cyclic load was applied to three specimens while one was tested under monotonic loading to provide data for the calibration of the analytical models. The moment-rotation hysteresis loops and the failure modes for all test specimens are presented. A full three-dimensional finite element model is also developed for each test specimen for use to predict their behavior and to provide a tool for generating subsequent extensive parametric studies. The test results show that all specimens performed well in terms of rotation capacity and strength. Finite element models are found to be capable of approximating the cyclic behavior of the extended end-plate connection specimens.

**Keywords:** four-bolt unstiffened moment end-plate connection; cyclic performance; rotation capacity; finite element model

---

### 1. Introduction

Since the Northridge and Kobe earthquakes, a number of researches have been conducted to investigate the response of connections and behavior of steel moment-frame buildings under monotonic and cyclic loading conditions. With the developments obtained through these researches a number of connection details have been revised and improved to achieve acceptable performance for use at high seismic demands. The revised specification provisions require that beam-to-column moment connections be designed with sufficient strength to force development of the plastic hinge away from the column face to predetermined location within the beam span. In addition, all elements of the connection are required to have adequate strength to develop the forces resulting from the formation of the plastic hinge. These connections designed by incorporating the provisions adopted are classified as prequalified. Prequalification test results for the extended end-plate moment connections can be found in Meng (1996), Meng and Murray (1997), Ryan and Murray (1999), Sumner *et al.* (2000a, b), Sumner and Murray (2001a, b), and

---

\*Corresponding author, Ph.D. Student, E-mail: [ilkerakgonen@hotmail.com](mailto:ilkerakgonen@hotmail.com)

Sumner and Murray (2002).

Many numerical and experimental studies were also carried out on end-plate moment connections composed of European steel shapes. Nogueiro *et al.* (2006) studied behavior of standardized European end-plate beam to column steel joints under monotonic and arbitrary cyclic loading. Generation of moment-rotation curves was presented. Bolted beam-column connections with extended end plate made up of the high strength steel S690 was examined by Girão Coelho *et al.* (2007). The parameters investigated were the extended end-plate thickness and bolt grade for beam-to-column connections with typical European sections. Shi *et al.* (2008) has performed a numerical simulation of steel pre-tensioned bolted end-plate connections of different types and details. Numerical model including geometric and material non-linearity was validated well against test results. FE analyses have also provided additional results which are difficult to measure in physical tests, such as friction between end-plate and column flange and distribution of pressure caused by bolt pretension. Gerami *et al.* (2010) has investigated the cyclic behavior of bolted connections with different arrangements of bolts. FE model is used to analyze and to compare the cyclic behavior of T-stub and end-plate connections by changing the vertical and horizontal arrangement of bolts. Test results showed that initial rotational stiffness and moment capacity of T-stub connections were obtained higher than end-plate connections. Diaz *et al.* (2011) has developed a FE model of beam to column extended end-plate joints. Moment-rotation curve obtained from FE model including geometric and material non-linearity was validated with experimental results found in literature. Procedure for determining the moment-rotation curve using FE model was also given with details. Abidelah *et al.* (2012) has conducted the research including experimental and analytical behavior of bolted end-plate connection with or without stiffener. Four of the connections were detailed with stiffeners. Column elements were designed weaker than beam elements in order to observe failure mode at tension and compression zone. Experimental results such as failure mode, moment-rotation curves, and rigidity were compared with the analytical results given by Eurocode3 (CEN2003). Dessouki *et al.* (2013) studied the behavior of I-beam bolted extended end-plate moment connections. A three-dimensional FE model was used to examine the non-linear behavior of extended end-plate connections. Yield line patterns and distribution of stresses in the end-plates were analyzed for four bolts and multiple row extended end-plates using FE model.

ANSI/AISC 358-10 has presented the prequalified connection types with some parametric limitations regarding geometrical dimensions of the elements constituting the connection, such as beams, columns, end plates and bolts. Prequalified connections are demanded to be used in special moment frames (SMF) and intermediate moment frames (IMF) systems in accordance with the provisions specified in ANSI/AISC 341-10. AISC Design Guide 4: Extended End-Plate Moment Connections also provides design procedures and design examples for the extended end-plate moment connection configurations classified as prequalified.

Significant revisions were introduced into the Turkish Earthquake Code (TEC) in 2007 for the steel buildings. These changes were largely based on USA design codes and practice. In current seismic design code (TEC (2007)), steel moment frames are classified as systems of either highly ductile moment resisting frames corresponding to special moment frames (SMF) or nominal ductile moment resisting frames corresponding essentially to ordinary moment frames (OMF) and partially intermediate moment frames (IMF) based on detailing of connections. The prequalified connection details for SMF systems have only been addressed in TEC (2007).

Steel moment frames can incorporate a number of different types of beam-to-column connections to be able to sustain their performance without significant degradation under seismic

loading. The extended end-plate connections which have proved to be very effective in transmitting significant amount of moments have been widely used in Turkey. The behavior of this type of connection can be controlled by a number of different limit states including flexural yielding of the beam section, flexural yielding of the end-plate, yielding of the column panel zone, tension rupture of the bolts, shear rupture of the bolts, or rupture of the welds. Details for two moment extended end-plate connection configuration, designed as four-bolt unstiffened and eight-bolt stiffened, are presented as prequalified connections in TEC (2007). The range and type of parameters for the connection prequalification, specified in this code, are similar with some differences to USA codes and practice. For example, in ANSI/AISC 358-10, size and flange thickness of beam, size and thickness of the end-plate, bolt gauges are considered as design parameters of the connection; however, in TEC (2007) these parameters are not taken into account for connection design purpose. In addition, European structural steel grade and European steel sections which are very popular in Turkey differs from size of W sections employed in USA. To use the design procedure recommended by AISC Design Guide 4, this study was planned to explicate the seismic characterization and validation of current provisions necessitated by TEC (2007) for the behavior of the four-bolt unstiffened moment end-plate connections defined as prequalified connections.

In this paper, cyclic performance of the four-bolt unstiffened moment end-plate connection, representing an exterior joint sub-assembly, designed with European steel sections made of S275 steel was investigated in terms of rotation capacity and strength. The flange widths and depths of the beams used for the connection specimens fell out of the parametric limitations required by ANSI/AISC 358-10. In first phase of the study, one specimen was tested under monotonic loading to provide data for the calibration of the finite element models of the specimens. Then, in second phase, cyclic loading was applied to each three specimen. The experimental test results are presented and discussed through the comparison made between the test results and analytical results obtained from the models in the following sections.

## **2. Description of the test program**

### *2.1 Design of test specimens*

Four connection specimens were prepared in order to evaluate the geometrical limitations specified in TEC (2007) and ANSI/AISC 358-10. The beam-column connections were made with four-bolt, extended, unstiffened end-plate connections. The column was designed to remain essentially elastic, resulting in HEB 320 section with 8 mm doubler plates and 20 mm continuity plates, while the beam sections of IPE 270 and HEB 180 were determined so as to allow the development of their plastic moments within the end region of the beam. The steel grade, specified for the beams and columns, was S275 while the end-plates, continuity plates and doubler plates were S235. Grade 10.9 bolts were employed in all specimens. The characteristics of the specimens were summarized in Table 1.

The width-to-thickness ratios for the flanges and web of the sections for all specimens conform to the requirements of the ANSI/AISC 341-10 and TEC (2007) seismic provisions. Both design codes recommend the same equation for the determination of the limiting slenderness ratio. For the compression elements of highly ductile members, limiting value of width-to-thickness ratios were determined as 6.62 for IPE 270 and 6.43 for HEB 180 steel shapes, respectively. Herein,

Table 1 Details of specimens

Specimen	Column	Beam	Bolt (Grade)	Loading type
P1	HEB320	IPE270	M22 (10.9)	Monotonic
P2	HEB320	IPE270	M22 (10.9)	Cyclic
P3	HEB320	IPE270	M24 (10.9)	Cyclic
P4	HEB320	HEB180	M24 (10.9)	Cyclic

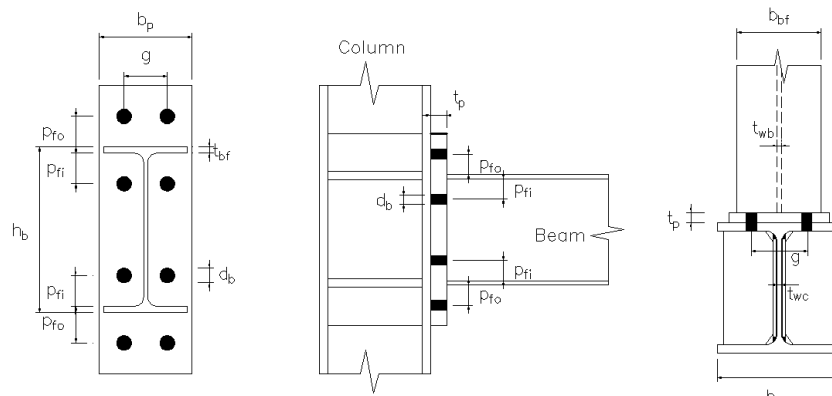


Fig. 1 Typical geometrical configuration of the four-bolt unstiffened end plate connection

yield stress and modulus of elasticity were assumed to be equal to 275N/mm<sup>2</sup> and 200000 N/mm<sup>2</sup>, respectively.

A typical geometrical configuration of the four-bolt unstiffened end plate connection is shown in Fig. 1. A comparison was made between TEC (2007) and ANSI/AISC 358-10 with respect to parametric limitations on prequalification of four-bolt unstiffened configuration of the specimens as shown in Table 2. The bold numbers in Table 2 indicate the incompatibility of the geometric limitations with those specified in ANSI/AISC 358-10 for the prequalification.

The end-plate was connected to the beam flange by complete joint penetration groove weld and to the beam web by fillet weld on both sides. Manual metal arc welding process with coated electrode was used. The minimum specified tensile strength of the weld metal (E7018) was 530

Table 2 Comparison of parametric limitations on prequalification of four-bolt unstiffened configuration

Parameters	TEC07		AISC 358-10		SPECIMENS			
	Min	Max.	Min.	Max.	P1	P2	P3	P4
$t_{bf}$	-	20	10	19	10.2	10.2	10.2	14
$b_{bf}$	-	-	152	235	<b>135</b>	<b>135</b>	<b>135</b>	180
$h_b$	-	750	349	1400	<b>270</b>	<b>270</b>	<b>270</b>	<b>180</b>
$t_p$	-	-	13	57	35	35	35	35
$b_p$	-	-	178	273	190	190	190	210
$g$	-	-	102	152	120	120	120	120
$P_{fi}, P_{fo}$	-	-	38	114	50	50	50	50

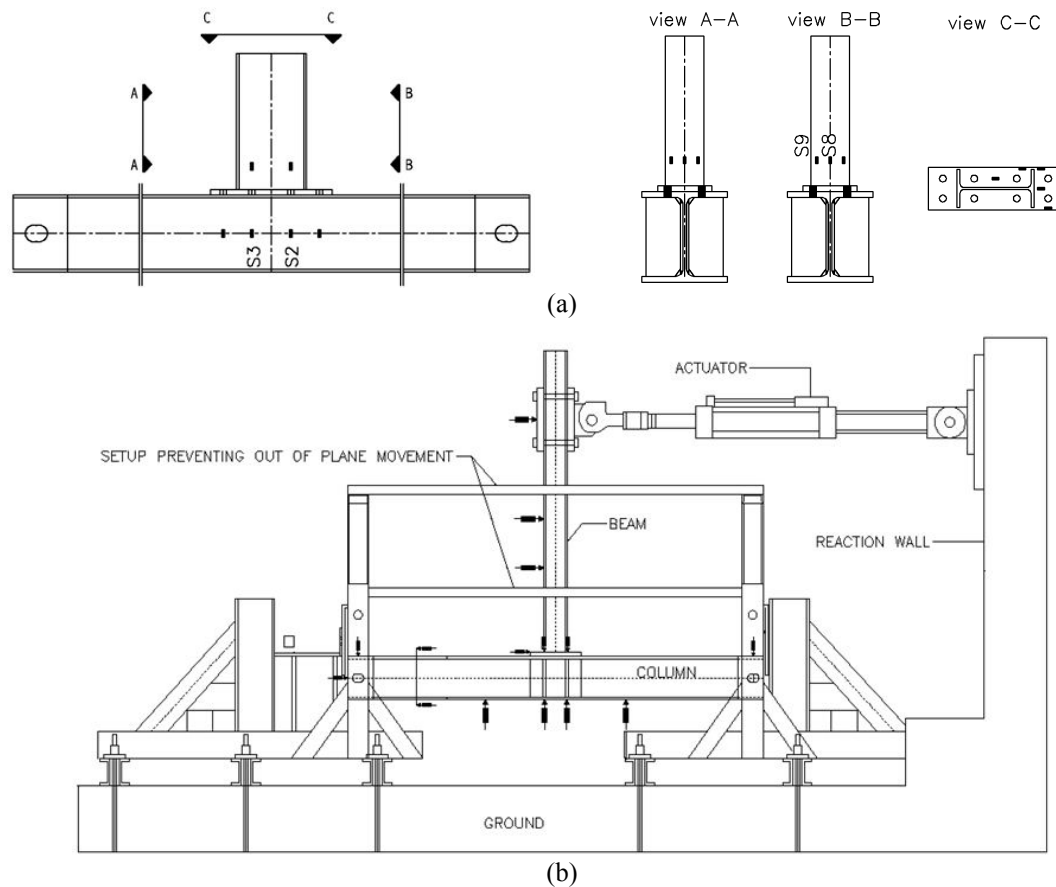


Fig. 2 (a) Instrumentation of specimens; (b) Test setup

$\text{N/mm}^2$ . Bolts were pre-tensioned up to 70% of their ultimate tensile capacity.

The connection specimens were designed to develop the expected plastic moment capacity of the connected beams. Thus, column, end-plate, bolts and welds used in the specimens were provided to essentially remain elastic during the tests. Plastic deformation was aimed only at plastic hinge away from the column face within the region of beam end.

Specimen P1 was only subjected to monotonic loading. Three of the four specimens were subjected to displacement cycles of increasing amplitude. Specimen P2 was identical to specimen P1 except that it was subjected to cyclic loading rather than monotonic loading. Specimens P1, P2 and P3 were designed with a beam section of IPE 270 and HEB 180 was used as the beam in design of Specimen P4. Both beam sections have almost same plastic section modulus, resulting in the same plastic moment capacity. This was done so in order to observe the effect of the connection configuration on the cyclic performance depending on the dimensional properties of the connected beams.

## 2.2 Experimental setup, instrumentation and loading

Four test specimens consisted of extended end plate connections, denoted P1, P2, P3 and P4,

Table 3 Cyclic displacement history

Load step	Peak deformation, $\Theta$	Number of cycles, $n$
1	0.00375	6
2	0.005	6
3	0.0075	6
4	0.01	4
5	0.015	2
6	0.02	2
7	0.03	2

\*Continue with increments in  $\Theta$  of 0.01 rad., and perform two cycles at each step

were designed for monotonic and cyclic testing. The height of the column is 3.0 m. The columns of all specimens have web transverse stiffeners at the level of the beam flanges, and cantilever beam length is 2.0 m. The out-of-plane deformation of the specimens was restrained during the tests. The displacement cycles applied at the tip of the beam was provided by a hydraulic actuator capable of producing up to force of 250 kN. No any axial force on beam and column is applied.

Test specimens were instrumented with displacement transducers and strain-gauges. Each specimen was mounted to the test setup in such a way that the beam was in vertical position and the column was placed in horizontal plane, as shown in the Figs. 2(a) and (b). The connection regions of all specimens were painted with white wash in order to observe yield formations. The full experimental set up for an exterior joint sub-assembly and the arrangement of the instrumentation are also shown in Figs. 2(a) and (b).

ATC-24 Protocol (ATC-24, 1992) and SAC Protocol (Clark *et al.* 1997) are two widely used loading protocol for testing of steel sub-structures. Both protocols use different control parameter for determination of cycle amplitudes. While ATC-24 Protocol uses yield displacement as a control parameter, SAC Protocol considers story drifts rather than yield deformation. Because of the ambiguity for determination of exact yield point, ATC-24 Protocol possesses a major difficulty for application. For this reason, SAC Protocol was preferred for testing of the specimens. SAC Protocol loading steps and the number of cycles for each can be seen from Table 3. Each load step corresponds to a total interstory drift angle.

Table 4 Coupon test results

Coupons	Modulus of elasticity, $E$ (N/mm <sup>2</sup> )	Yield stress $F_{y,act}$ (N/mm <sup>2</sup> )	Elongation at yield $\epsilon_y$ (average)	Tensile strength $F_{u,act}$ (N/mm <sup>2</sup> )
IPE270	199881	337.25	0.001687	454.86
HEB180	203507	306.13	0.001504	450.02
PL8	209470	317.00	0.001513	456.05
PL20	210230	313.26	0.001490	449.88
PL35	212477	401.00	0.001887	533.14
HEB320	206669	293.00	0.001418	456.36

### 2.3 Material tests

Two tensile dog bone coupons cut from end plate sheet and steel profiles were tested in accordance with EN10002-1. Coupons were taken from flange of the beams and columns. The average actual nominal values for the beams, end plate, and column are set out in Table 4. Steel grade preferred for column and beam profiles was S275 with nominal minimum yield stress,  $F_{y,nom}$  and nominal minimum tensile strength,  $F_{u,nom}$  of 275 N/mm<sup>2</sup> and 430N/mm<sup>2</sup>, respectively. The structural steel for end plates was S235 with nominal minimum yield stress,  $F_{y,nom}$  and nominal minimum tensile strength,  $F_{u,nom}$  of 235N/mm<sup>2</sup> and 360 N/mm<sup>2</sup>, respectively. The results of the coupon tests showed that the experimental values were higher than the nominal ones. The coupon test results were used in determining the actual moment capacity of the beam.

### 3. Modeling of the specimens

It is well known that experimental researches on connections are very expensive and mostly impractical for engineers. Therefore, interest on simulations is increasing in parallel with advancing computer technology. Simulation study provides easiness and speed for performing numerous analyses with different geometries and material properties without cost. However, these types of models also needed to be verified based on experimental results. Herein, a monotonic test was used to verify the Finite Element Models (FEMs) and details of the verification are given in the sections below. In the simulation studies, FEMs of the specimens were created using the software package ANSYS.

FEMs were developed without utilizing symmetry property. Several mesh models with different sizes were tried for numerical model; consequently, mesh model was established using patch confirming method. All members were meshed using 10 node quadratic tetrahedron element (SOLID187) as shown in Fig. 3. The contact interaction between column flange and extended end plate was simulated by quadratic triangular contact element (CONTA174) and quadratic triangular target element (TARGE170). The contact and target elements are able to represent a deformable contact surface with friction and sliding effect. Friction coefficient between column flange and end plate was applied as 0.44. This value was determined based on the data obtained from monotonic

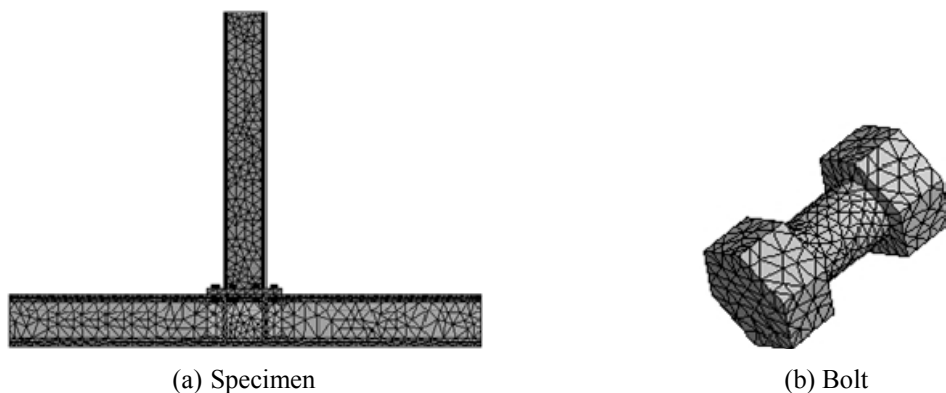


Fig. 3 Meshing of FEM

test results. Bolt pre-tension loading was modelled using (PRETS179) element within the meshed model of bolt shanks. Detailed information of these elements can be found in ANSYS element reference.

Tension test results for yield stress and elastic modulus from the material test data for the end plates, beams and columns described above were used for the material properties. Kinematic hardening model was adopted to represent the stress-strain behavior of all steel members' material. Poisson ratio of steel was taken as 0.3. Von Mises yield criterion was applied to investigate yielding of materials. Tangent modulus at the plastic region was taken as 10 MPa for all materials. This was done so to avoid convergence problems in the analyses.

Analysis was divided into two stages similar to experimental study. First, boundary conditions were applied at the end of column and then bolts were pre-tensioned with an equivalent force of approximately 70% of the ultimate tensile strength of the bolt. After the completion of the first step, a monotonically increasing lateral displacement load was applied at the tip of the beam. P-delta effect was considered with using large displacement static analysis.

### 3.1 Verification of FEMs

The moment-rotation curve of the Specimen P1 obtained by the test results was used for the verification of the models. The moments obtained from experimental tests are obtained using the

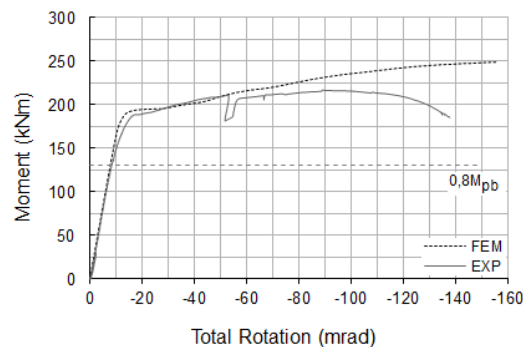


Fig. 4 Comparison between the test results and FEM of Specimen P1

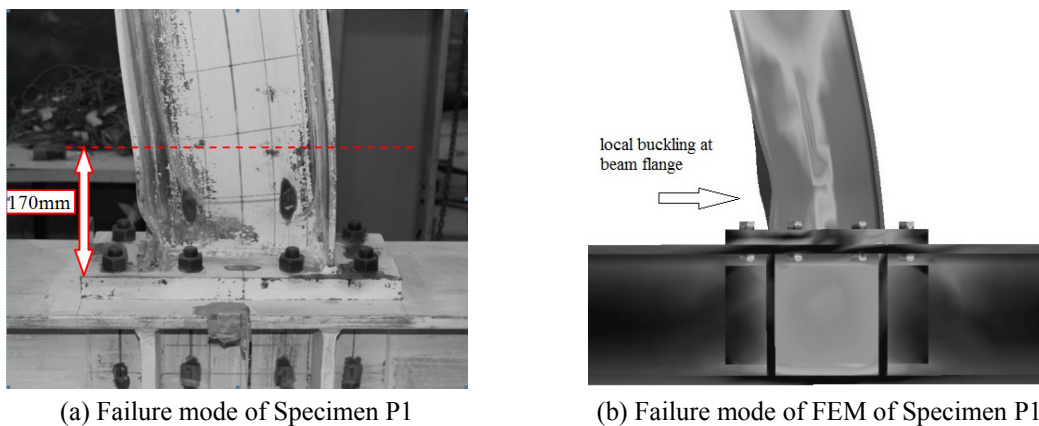


Fig. 5 Comparison of failure modes of Specimen P1

measured load at the actuator and the lever arm from the point at which the actuator was mounted to the column center line. Fig. 4 shows the moment-rotation relationship obtained from the test and the FEM analysis of the Specimen P1 under monotonic loading. Because of power cutting experienced during the test, a sudden loss of load occurred as can be seen in Fig. 4. Fig. 4 shows a good agreement between the moment-rotation curve of the test results and FEM. The moment-rotation behavior of the Specimen P1, therefore, was adequately simulated by the FEM. The failure mode of Specimen P1 observed during the test was the local buckling of the beam flange and web in the compression. As can be seen from Fig. 5, the failure modes observed in the test and the FEM analysis are found to be in good agreement.

#### **4. Experimental observations and evaluation**

For a four-bolt unstiffened extended end-plate connection for which their details are presented in Table 1, the experimental observations made during the tests (i.e. the failure modes, ultimate moment strength, rotations limits) are presented below.

Specimen P1 was subjected to monotonic loading. It was horizontally loaded at the tip of the beam up to displacement of 13.23 mm that corresponds to the load of 41.4 kN (79.7 kNm) and a nearly half of the elastic limit. After this level, specimen was totally unloaded and then horizontal load applied until the failure of the specimen. Whitewash flaking observed on beam web near end plate indicates onset of yielding at the displacement level of 30.00 mm which corresponds to 87.4 kN (168.25 kNm). Initial stiffness of the specimen was found to approximately be 52389 kN/mrad. The ultimate moment was obtained from the results of Specimen P1 as 216.91 kNm (112.678kN). Local buckling zone of beam flange was observed at 170 mm away from the end-plate face.

Specimen P2 was identical to Specimen P1 except that cyclic loading was applied rather than monotonic loading. Specimen P2 behaves elastically up to displacement of +19.05 mm and -19.05 mm, which corresponds to +83.637 kN (159.33 kNm) and -84.63 kN (161.22 kNm), resulting in 0.01 rad. Initial stiffness of the specimen was found to nearly be 57548 kN/mrad. The moments were +231.91 kNm in the tension and -245.34 kNm in the compression at the end of 0.04 radian cycles. Strength degradation due to local buckling of beam flange was observed at 0.05 radian cycles. Test was terminated when the rupture of beam flange occurred. The cycles of SAC protocol were completed without failure at displacement of 114.3 mm which corresponds to 0.06 rad. Plastic hinge zone was indicated by flaking the whitewash as shown in Fig. 6(a) and was observed at almost 75-110 mm far away in distance from end-plate face at the end of the test. As can be seen from the failure modes shown in the Figs. 6(a) and (b), the FEM results have good agreement with the experimental one at the different stages of loading.

Specimen P3 was identical to Specimen P2 except bolt size. The specimen performed elastic behavior up to displacement of +18.95 mm and -18.95 mm, which corresponds to +81.813 kN (155.035 kNm) and -85.275 kN (161.6 kNm), resulting in 0.01 rad. Initial stiffness of the specimen was obtained roughly 59456 kN/mrad. The ultimate moments were 224.89 kNm (118.28 kN) and -245.58 kNm (-129.60 kN) at the end of 0.04 radian cycles. Strength degradation because of local buckling of the beam flange was observed at 0.05 radian cycles. Due to occurrence of complete rupture of the beam flange test was terminated at 75% of 0.07 radian cycles. Plastic hinge zone was formed approximately at 75-110 mm away from the end-plate face. The deformation of beam flanges corresponding to the mode of failure is shown in Figs. 6(c) and (d) for Specimen P3.

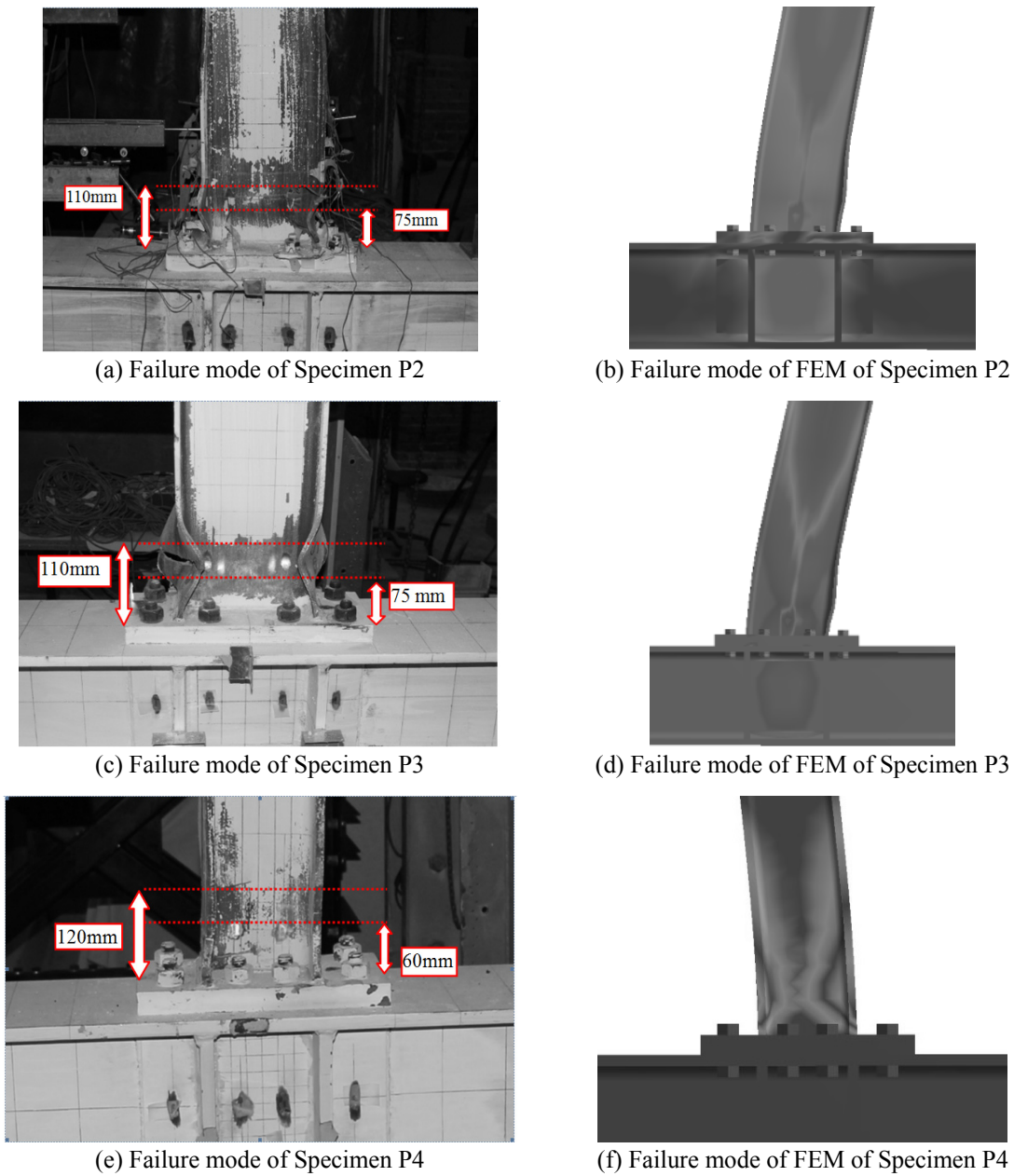


Fig. 6 Deformation of beam flanges for specimens P2, P3 and P4

Specimen P4 exhibited elastic behavior up to displacement of +18.8 mm and -18.8 mm which corresponds to +64.94 kN (121.96 kNm) and -65.24 kN (122.52 kNm), resulting 0.01 radian. Initial stiffness of roughly 47292 kN/mrad was achieved for the specimen. The highest values of the moment were recorded as +233.44 kNm (124.30 kN) and -250.53 kNm (-133.41 kN) for the specimen at the end of 0.07 radian cycles without failure. Test was terminated at 25% of 0.08 radian cycles. No serious local buckling at the beam and strength degradation was observed before

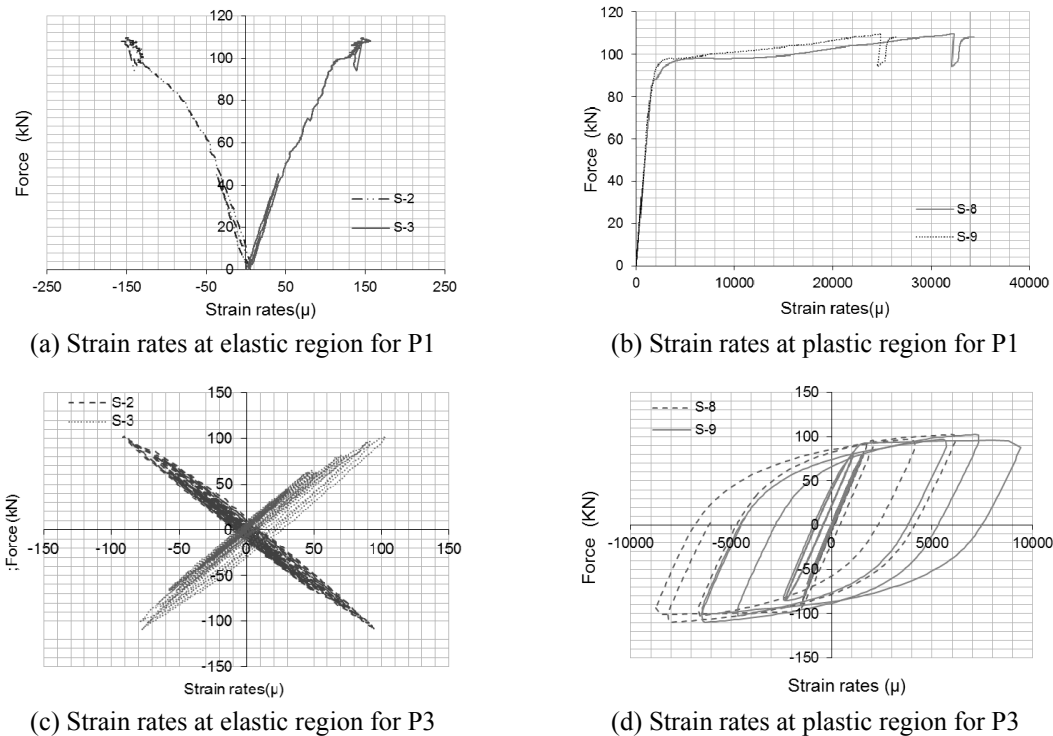


Fig. 7 Strain-gage curves from experimental studies under monotonic and cyclic loading

the last cycle. Plastic deformation zone was formed nearly at 60-120 mm away from end-plate face as shown in Fig. 6(e). The deformation of beam flanges corresponding to the mode of failure is shown in Figs. 6(e) and (f) for Specimen P4.

In general, the cyclic test results show that plastic hinges occurred at the beam end and there were no indications of plastic deformations in the column flanges, end-plate, bolts and welds during the tests for all specimens. According to the test results, if the beam has less compact flanges, a plastic hinge may take place at a section nearer the beam end than it was expected for a beam with more compact flanges. In case of more compact beam flanges that corresponds to use of HEB 180 herein, the location distance of the plastic hinge was measured as nearly 90 mm ( $h_b / 2$ ) from the face of the end plate. This distance was obtained again as approximately 90 mm ( $h_b / 3$ ) for IPE 270, where  $h_b$  is the depth of the beam. Typically, strain-gage curves from experimental studies under monotonic and cyclic loading are shown in Fig. 7 for the beam flange and column web of Specimen P1 and Specimen P3. As can be seen from the Figs. 7(a) and (c), the beam-to-column joint panel zone has remained elastic throughout the test. However, Figs. 7(b) and (d) shows that the beam flange has reached yield as expected.

## 5. Comparison and discussion

It is well known that a moment connection of the steel moment resisting frames designed as a seismic force resisting system must develop a minimum total rotation (inter-story drift angle) of 40

mrad which is recommended by FEMA 350 and TEC (2007) for special moment frames to ensure desired ductile behavior. Also, the seismic provisions require that the measured flexural strength of the connection shall be at least  $0.8M_{pb}$  of the connected beam at an inter-story drift angle of at least 40 mrad, where  $M_{pb}$  is the nominal plastic moment strength of the beam, calculated using the specified minimum yield stress. Although strength degradation was observed in Specimen P2 and P3, moment strength of joints always remained more than  $0.8M_{pb}$  indicated by dashed lines in Fig. 8. Experimental research showed that all specimens satisfied the required minimum total rotation capacity criteria specified in ANSI/AISC 358-10.

Moment-rotation curves from the test results are also compared with the analyses results of the models as shown in Figs. 8(a), (b) and (c) for Specimen P2, P3 and P4, respectively.

Moment-rotation curves of Specimen P2 and P3 are satisfactorily simulated by their models in elastic region as shown in Figs. 8(a) and (b), respectively. In inelastic region, the ultimate capacities of the connections that correspond to the rotation of 40mrad were satisfactorily predicted although strength degradation due to local buckling of the flanges was not sufficiently represented by the models. Additionally, while the kinematic hardening model adopted for steel material provided good accuracy in the simulation of Specimen P4's cyclic response, the use of that model for Specimen P2 and P3 caused inadequacies exhibited by the FEMs. This comparison revealed that the connected beam sections with flanges more susceptible to local buckling was more sensitive to steel material hardening model to be considered in FEMs. Furthermore, strength degradation because of local buckling, which could not be accurately represented by FEMs, increased the discrepancies between the curves. Despite of these, the moments of the connections

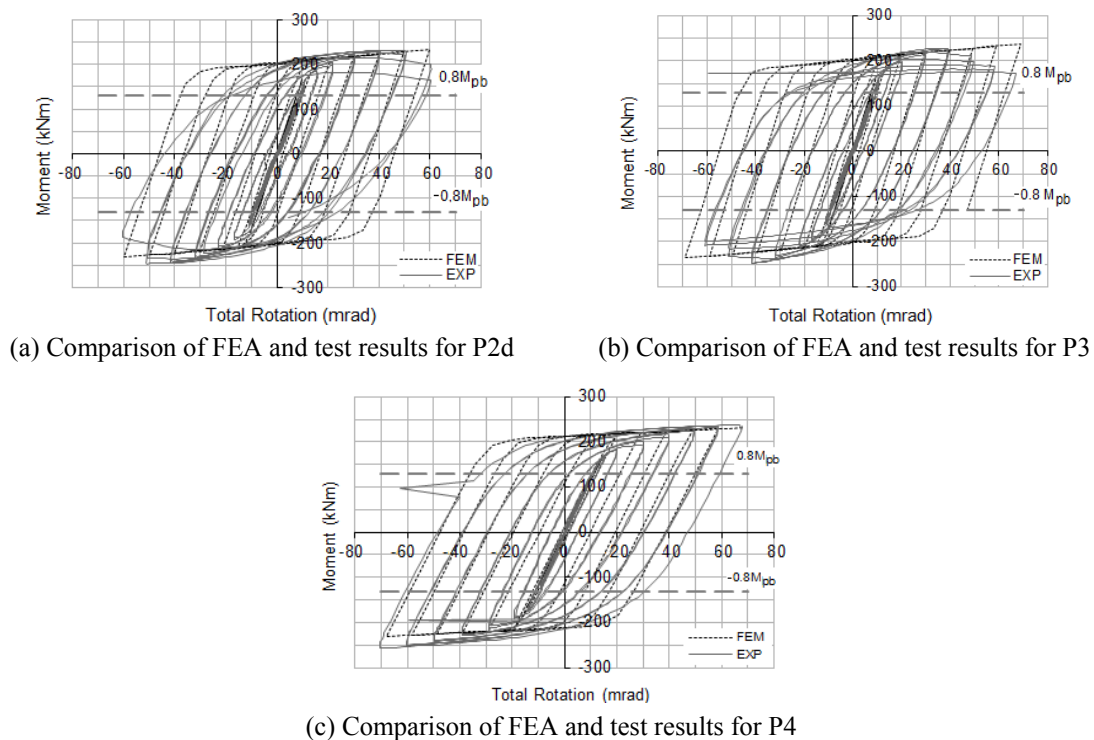


Fig. 8 Comparison of moment-rotation curves for FEA and cyclic test results

predicted by the FEMs at the inter-story drift angle of 40 mrad were in good agreement with the test results. The locations of the plastic hinge zones obtained from the FEM analyses were found to be very close to those from the tests results.

Moment-rotation curve of the Specimen P4 is shown in Fig. 8(c), where the hysteresis loops from the analysis has been superimposed. As can be seen from the figure, the cyclic behavior of the connection is adequately estimated by the model. There were no any indication of local buckling at the beam flanges and webs at the end of the test. The moment capacities of the Specimen P3 and P4 achieved in the tests were very close to each other with no considering the strength degradation experienced by the Specimen P3. This shows that the use of beam sections with more compact flanges would be more effective to avoid the possible strength degradation.

The behavioral characteristics of connections can be determined based on the three significant parameters such as ultimate moment strength ( $M_u$ ), initial stiffness ( $K_i$ ) and the applied maximum rotation capacity ( $\phi_u$ ). The ultimate moment strengths  $M_u^+$  and  $M_u^-$  are the maximum values of the connection moment during the whole cyclic loading procedure, not the maximum moment of the last load cycle.  $M_u^+$  and  $M_u^-$  are the positive and negative ultimate moment strengths, respectively, and it is positive when the load applied at the end of the beam is a pushing load, and it is negative when it is a pulling load. These parameters obtained from the connection specimens were summarized in Table 5.

To better understand the effect of the loading type on the connection behavior a comparison between Specimen P1 and P2 was made as shown in Fig. 9(a). From this figure, it is very clear to see the strength degradation from the cyclic loading at end of the test while this phenomenon was not observed in monotonic loading. The ultimate moment strength achieved in the cyclic test was larger than that from the monotonic test due to the stress-strain relationship of the steel material under effect of the cyclic loading that requires the consideration of the cyclic inelastic strain behavior of the material. However, a good agreement was obtained between yield moments. Considering the local buckling of the beam flanges, failure modes of the specimens are similar to each other. Initial stiffnesses of the specimens are found to be very close to each other. However, while formation of plastic hinge zones can be observed clearly in cyclic tests, monotonic test cannot be satisfactorily used to determine the location of plastic hinges. Although the depth of the beam and the width of the beam flange are not compatible with the limitations specified in ANSI/AISC 358-10, Specimen P2 exhibited desirable performance in terms of moment capacity and rotation capacity. The ultimate moment capacity was larger than  $0.80M_{pb}$  at 40 mrad and the maximum rotation of 60 mrad was achieved without considerable strength degradation as shown in Fig. 8 (a).

Table 5 Properties of specimens

Specimen	$K_i$ (kN/mrad)	$M_u$ (+) (kNm)	$M_u$ (-) (kNm)	$\Phi_u$ (mrad)	Loading type	Failure mode
P1	52389	216,91	-	138,3	Mon.	Local buckling at beam flange
P2	57548	231,91	-245,34	60	Cyc.	Local buckling at beam flange, rupture at beam flange.
P3	59456	224,89	-245,58	60	Cyc.	Local buckling at beam flange, rupture at beam flange
P4	47292	233,44	-250,53	70	Cyc.	Local buckling at beam flange

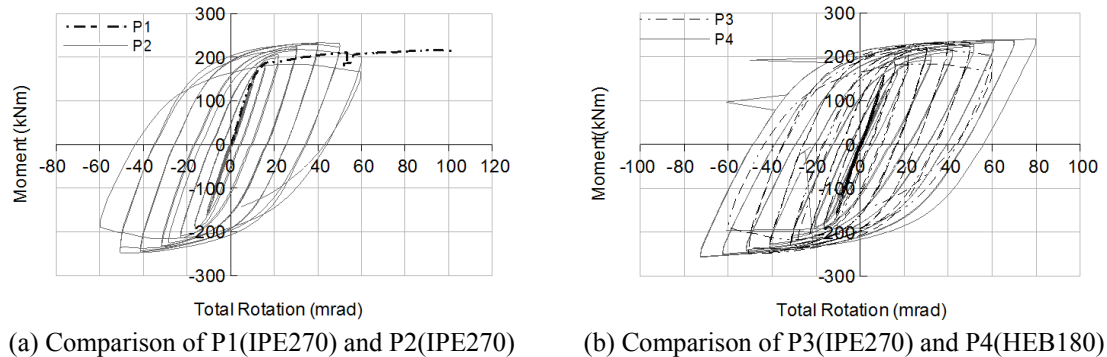


Fig. 9 Comparison of experimental test results

Specimen P3 is identical to Specimen P2 except for bolt diameter as can be seen from Table 1. These two specimens exhibited similar behavior as expected. Strength degradation for Specimen P2 and Specimen P3 started just after 40 mrad rotation. Both specimens are found to be satisfactory with the capability to have the strength and the rotation capacity.

Specimen P3 and P4 were considered to see the behavioral difference between the connections composed of beam sections with the almost same plastic section modulus and different dimensional properties. Therefore, Specimen P3 was designed with the steel shape of IPE 270 while Specimen P4 had a beam with HEB 180. Hysteretic response of the Specimen P4 exhibited very stable behavior with wide hysteretic “S” shapes is shown in Fig. 9(b). The main difference between the hysteresis of Specimen P3 and P4 is that no any strength degradation was observed in the Specimen P4. This is attributed to that the flange of the HEB 180 was more compact than that of IPE 270. Thus, local buckling of the flanges of HEB 180 that was expected to cause strength degradation as in the Specimen P3 did not occur until the end of the test. However, initial stiffness value of the Specimen P4 was lower than that of the Specimen P3 due to larger flexural rigidity of IPE 270.

### 5.1 Evaluation of over-strength factor

In conventional design, the required moment capacity is determined based on the nominal yield stress which is lower than the actual stress performed by the steel material. In capacity-based design, it is obviously important to be able to calculate over-strength amount of flexural members for the forces to be considered in design of the elements comprising a connection. Therefore, seismic design codes essentially deal with the expected over-strength in yielding to provide the ductile behavior. Herein, the beam-to-column connection elements of the specimens were designed as to transmit the forces resulting from the moments at the plastic hinges within the beam. The expected plastic moment strength of the beam,  $M_{pe}$  can be calculated as follows (ANSI/AISC 358-10).

$$M_{pe} = R_y C_{pr} F_y Z_x = R_y \left( \frac{F_y + F_u}{2F_y} \right) F_y Z_x \quad (1)$$

where  $Z_x$  is plastic section modulus and  $F_y$  is a specified minimum yield stress of a beam.  $C_{pr}$  is a factor accounting for the peak connection strength, including strain hardening, local restraint, and

other possible sources of over-strength. This factor can directly be taken as 1.1 according to TEC (2007) while it is computed depending on the yield stress and tensile strength in ANSI/AISC 358-10. The ratio of expected yield stress to the specified minimum yield stress,  $R_y$  is specified as 1.1 in TEC (2007) for hot rolled structural shapes with S275. Consequently, in TEC (2007), the cumulative material over-strength value is computed as 1.21 ( $= 1.1 \times 1.1$ ) for the steel grade S275. The ratio of expected tensile strength to the specified minimum tensile strength,  $R_t$  is not defined in TEC (2007).

To evaluate the range of expected yield stress and tensile strength for steel materials used in the test,  $R_y$  and  $R_t$  values were obtained based on the nominal yield stress, tensile strength and their actual values determined experimentally. The nominal yield stress of the structural steel,  $F_{y,nom}$  was 275 N/mm<sup>2</sup> and tensile strength,  $F_{u,nom}$  was 410 N/mm<sup>2</sup> for the beams tested. Based on the tensile test results, the values of  $R_{y,act}$  can be computed as 1.225 and 1.113 for IPE 270 and HEB 180, respectively, taking the ratio of the actual yield stress to the nominal yield stress. These ratios are found to be slightly larger than the specified value in TEC (2007). The ratios of  $C_{pr,act}$  can be determined as 1.175 for IPE270 and 1.235 for HEB180, respectively, using the actual yield stress and the actual tensile strength. Again, slightly larger  $C_{pr,act}$  than the specified one were obtained as shown in Table 6.

Specified minimum moment strength of the connection,  $M_{pe,nom}$  was initially calculated using cumulative over-strength factor ( $1.1 \times 1.1 = 1.21$ ) for all specimens according to TEC (2007). Considering only positive values given in Table 5, the maximum applied moments,  $M_u$  were compared with the expected moment strengths of the connected beams. A summary of the results is shown in Table 7.

The ratio of maximum applied moment,  $M_u$  to expected moment strength,  $M_{pe,nom}$ , which may be defined by  $R_y \times C_{pr}$ , ranges from 1.347 to 1.457. All these ratios are found to be larger than the specified cumulative over-strength factor that was determined as 1.21 for S 275 steel in accordance with TEC (2007).

Table 6 Evaluation of  $C_{pr}$  factor

Coupons	Yield stress, $F_{y,act}$ (N/mm <sup>2</sup> )	Tensile strength, $F_{u,act}$ (N/mm <sup>2</sup> )	$R_{y,act} = \frac{F_{y,act}}{F_{y,nom}}$	$R_{t,act} = \frac{F_{u,act}}{F_{u,nom}}$	$C_{pr,act} = \frac{F_{y,act} + F_{u,act}}{2F_{y,act}}$	$\frac{C_{pr,act}}{C_{pr}}$
IPE 270	337	455	1.225	1.109	1.175	0.943
HEB180	306	450	1.113	1.097	1.235	0.991

Table 7 Comparison of expected and actual moment capacity of connecting beam

Test	$M_{pe,nom}$ (kNm)	$M_u$ (kNm)	$\frac{M_u}{M_{pe,nom}}$
P1 (IPE 270)	161.05	216,91	1.347
P2 (IPE 270)	161.05	231,91	1.440
P3 (IPE 270)	161.05	224,89	1.396
P4 (HEB180)	160.18	233,44	1.457

\*( $M_u(+)$  positive moment in cyclic loading for P2, P3 and P4, see Table 5)

## 6. Conclusions

The primary goal of this research was to examine the conformity of the four-bolted unstiffened extended end-plate connections with European steel shapes made of S275 steel grade to the requirements of seismic applications recommended by ANSI/AISC 358-10. For this, three beam-to-column connection specimens were tested under cyclic loading while one, used for the verification of the FEMs of the specimens, was subjected to monotonic loading. None of the beams of the specimens complied with some parametric limitations on prequalification recommended by ANSI/AISC 358-10 such as beam flange width and overall depth. The behavior of the connection specimens were evaluated considering significant characteristics such as moment strength, initial stiffness, and rotation capacity using numerical and experimental methods. Following conclusions from this research can be drawn:

- Test results especially demonstrate that the specimens satisfy the current design provisions to achieve reasonable rotation and the moment strength demands.
- The performance of S275 steel is found to be satisfactory. However, test results showed that the cumulative material over-strength factor to be used in seismic design should be greater than 1.21 for S275 steel material.
- Test results also demonstrated that the degree of the beam flange compactness may influence the locations of the plastic hinges expected to occur at the beam ends. According to the test results, the plastic hinge of the beam with more compact flange formed at a farther distance from the end than did that of the beam composed of less compact flanges.
- Good agreement between the test results and analytical results is observed. The FEMs predicts the both the initial stiffness and the point of yielding accurately.
- Further researches based on the different parametric limitations required by ANSI/AISC 358-10 are obviously needed to widen the extent of these geometrical limitations specified for the members comprising the extended end-plate connections.

## Acknowledgments

The research was financially supported by Istanbul Technical University, Graduate School of Science Engineering and Technology. The assistance provided by Rozak Inc., in preparing test specimens is also greatly appreciated.

## References

- Abidelah, A., Bouchair, A. and Kerdal, D.E. (2012), "Experimental and analytical behavior of bolted end-plate connections with or without stiffeners", *J. Construct. Steel Res.*, **76**, 13-27.
- AISC Design Guide 4 (2003), *Extended End-Plate Moment Connections, Seismic and Wind Applications (Second Edition)*, American Institute of Steel Construction, Chicago, Illinois.
- ANSI/AISC 341-10 (2010), *Seismic Provisions for Structural Steel Buildings*, American Institute of Steel Construction; Chicago, IL, USA.
- ANSI/AISC 358-10 (2010), *Prequalified Connections for Special and Intermediate Steel Moment Frames for Seismic Applications*, American Institute of Steel Construction; Chicago, IL, USA.
- ANSYS (2007), Swanson Analysis Systems online manual, version 11.0, and theory reference.
- Clark, P., Frank, K., Krawinkler, H. and Shaw, R. (1997), "Protocol for fabrication, inspection, testing, and documentation of beam-column connection tests and other experimental specimens", SAC Steel Project

- Background Document; Report No. SAC/BD-97/02, October.
- Dessouki, A.K., Youssef, A.H. and Ibrahim, M.M. (2013), "Behavior of I-beam bolted extended end-plate moment connections", *Ain Shams Eng. J.*, **4**(4), 685-699.
- Diaz, C., Victoria, M., Marti, P. and Querin, O.M. (2011), "FE model of beam-to-column extended end-plate joints", *J. Construct. Steel Res.*, **67**(10), 1578-1590.
- EN 10002-1, (2001) Tensile testing. Part 1: Method of test at ambient temperature, European Committee for Standardization; Brussels, Belgium.
- FEMA-350 (2000), Recommended Seismic Design Criteria for New Steel Moment-Frame Buildings, SAC Joint Venture for the Federal Emergency Management Agency; Washington, D.C., USA.
- Gerami, M., Saberi, H., Saberi, V. and Daryan, A.S. (2011), "Cyclic behavior of bolted connections with different arrangement of bolts", *J. Construct. Steel Res.*, **67**(4), 690-705.
- Girão Coelho, A.M. and Bijlaard, F. (2007), "Experimental behavior of high strength steel end-plate connections", *J. Construct. Steel Res.*, **63**(9), 1228-1240.
- Meng, R. (1996), "Design of moment end-plate connections for seismic loading", Doctoral Dissertation; Virginia Polytechnic Institute and State University, Blacksburg, VA, USA.
- Meng, R.L. and Murray, T.M. (1997), "Seismic performance of bolted end-plate moment connections", *Proceedings of the 1997 National Steel Construction Conference*, Chicago, IL, USA, May, 30-1-30-14.
- Nogueiro, P., Simões da Silva, L., Bento, R. and Simões, R. (2006), "Experimental behaviour of standardised european endplate beam-to-column steel joints under arbitrary cyclic loading", *Stab. Ductil. Steel Struct.*, Lisbon, Portugal.
- Ryan, J.C. and Murray, T.M. (1999), "Evaluation of the inelastic rotation capability of extended end-plate moment connections", Research Report No. CE/VPI-ST-99/13 (Submitted to Metal Building Manufacturers Association, Cleveland, OH, USA; and American Institute of Steel Construction, Chicago, IL, USA, September).
- Shi, G., Shi, Y., Wang, Y. and Bradford, M. (2008), "Numerical simulation of steel pre-tensioned bolted end-plate connections of different types and details", *Eng. Struct.*, **30**(10), 2677-2686.
- Sumner, E.A. and Murray, T.M. (2001a), "Experimental investigation of four bolts wide extended end-plate moment connections", Research Report No. CE/VPI-ST-01/15; (Submitted to Star Building Systems, Inc., Oklahoma City, OK, USA, December), 114 p.
- Sumner, E.A. and Murray, T.M. (2001b), "Experimental investigation of the MRE 1/2 end-plate moment connection", Research Report No. CE/VPI-ST-01/14; (Submitted to Metal Building Manufacturers Association, Cleveland, OH, USA, December), 91 p.
- Sumner, E.A. and Murray, T.M. (2002), "Behavior of extended end-plate moment connections subject to cyclic loading", *J. Struct. Eng., ASCE*, **128**(4), 501-508.
- Sumner, E.A., Mays, T.W. and Murray, T.M. (2000a), "Cyclic testing of bolted moment end-plate connections", Research Report No. CE/VPI-ST-00/03; SAC Report No. SAC/BD-00/21; (Submitted to the SAC Joint Venture, May), 327 p.
- Sumner, E.A., Mays, T.W. and Murray, T.M. (2000b), "End-plate moment connections: test results and finite element method validation", *Connections in Steel Structures IV: Steel Connections in the New Millennium: Proceedings of the Fourth International Workshop*, Roanoke, VA, USA, October.
- Turkish Earthquake Code (2007), Specification for Buildings to be Built in Seismic Zones, Ministry of Public Works and Settlement Government of Republic of Turkey.